

# Alkylamine Assisted Ultrasound Exfoliation of MoS<sub>2</sub> Nanosheets and Organic Photovoltaic Application

Baodong Mao, Yongbo Yuan, Yuchuan Shao, Bin Yang,  
Zhengguo Xiao, and Jinsong Huang\*

*Department of Mechanical and Materials Engineering, University of Nebraska—Lincoln,  
Lincoln, NE 68588, United States*

The layered two-dimensional transition metal dichalcogenide MoS<sub>2</sub> have attracted great interest in electronic devices and energy conversion areas owing to its graphene like structure and superior optoelectronic properties. Here a liquid sonication method is developed for exfoliation of MoS<sub>2</sub> nanosheets with largely increased production yield by introducing alkylamines. The effect of alkylamine structure, initiating MoS<sub>2</sub> concentration and sonication time was investigated in terms of exfoliation yield and colloidal stability of the nanosheets. UV-vis absorption spectroscopy, transmission electron microscope, and Raman spectroscopy were used to characterize the exfoliated nanosheets. These MoS<sub>2</sub> nanosheets showed good dispersity in common organic solvents with good colloidal stability over months, which renders them the great potential for solution based device fabrication. Hybrid solar cell was constructed with MoS<sub>2</sub> nanosheets incorporating with polymer:fullerene as photoactive layer.

**Keywords:** MoS<sub>2</sub> Nanosheets, Transition Metal Disulfide, Two-Dimensional Layered Material, Ultrasound Exfoliation, Alkylamine, Organic Photovoltaics.

## 1. INTRODUCTION

Layered two-dimensional transition metal dichalcogenides, represented by MoS<sub>2</sub>, have attracted tremendous research interests owing to their fascinating electronic and optoelectronic properties.<sup>1–4</sup> Besides the graphene-like properties such as high carrier concentration, mobility and robust 2D structure, MoS<sub>2</sub> are superior to graphene due to the intrinsic band gaps (1.3 eV for bulk and 1.8 eV for monolayer) that enable more wide applications in electronics and optoelectronics.<sup>1,5</sup> MoS<sub>2</sub> nanosheets have been used in transistors,<sup>6,7</sup> phototransistors,<sup>8,9</sup> gas sensors,<sup>10</sup> and solar cells.<sup>11,12</sup> Recently MoS<sub>2</sub> is also widely studied for other energy conversion and storage applications, such as photocatalytic hydrogen evolution<sup>13–16</sup> and lithium ion batteries.<sup>17,18</sup>

Several classes of preparation methods have been developed for MoS<sub>2</sub> nanosheets, including mechanical exfoliation, chemical vapor deposition, liquid exfoliation and bottom-up solution synthesis, which consulted a lot from the methods of graphene.<sup>2,19</sup> Similar to graphene, mechanically exfoliated MoS<sub>2</sub> monolayers using tapes are still the main source for constructing high quality devices.<sup>6,20</sup> Lots of efforts are also contributed to chemical vapor deposition of wafer scale MoS<sub>2</sub> thin films for optoelectronic

device applications.<sup>21,22</sup> Among these methods, liquid exfoliation methods have been used most widely owing to the advantages of large scale production and low cost. To achieve liquid exfoliation of MoS<sub>2</sub> nanosheets, one strategy is ion intercalation of MoS<sub>2</sub> crystals using butyllithium<sup>23</sup> or sodium naphthalenide,<sup>24</sup> followed by mild ultrasonication in water. Ion intercalation method can produce MoS<sub>2</sub> monolayers in relatively large amount, but sometimes a post-synthesis treatment is needed to recover the electrical properties. The other strategy is direct exfoliating the MoS<sub>2</sub> crystals in suitable solvents by strong probe type ultrasonication.<sup>25</sup> The sonication assisted liquid-phase exfoliation method was originally developed for graphene<sup>26</sup> and has been applied to several classes of layered materials, such as transition metal dichalcogenides, *h*-BN, oxides, clays, and layered double hydroxides etc.<sup>25</sup> This method combines the advantages of physically exfoliated nanosheets with the good crystallinity and the large scale production potential of solution based methods. In the study by Coleman et al. series of solvents were systematically compared, where *N*-Methyl-2-pyrrolidinone (NMP) was found to be the best exfoliation media.<sup>27</sup> Lots of strategies, such as increasing sonication time,<sup>28</sup> grinding and balling,<sup>29,30</sup> and cosolvent design<sup>31</sup> have been explored to increase the production yield and to achieve size and thickness control of the

\*Author to whom correspondence should be addressed.

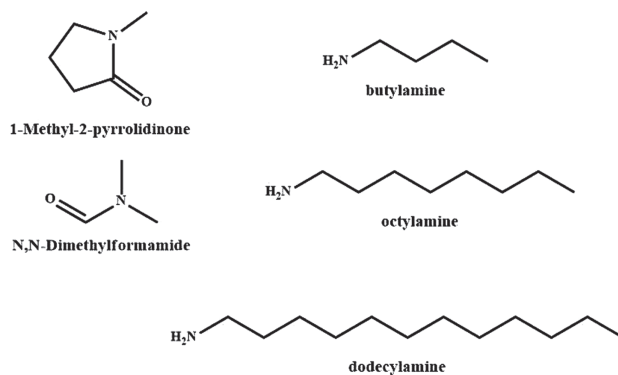
nanosheets. Polar solvents are more widely used in order to increase the production yield of the exfoliated nanosheets, especially water/alcohol mixtures,<sup>31</sup> surfactant solutions<sup>32</sup> and polymer solutions.<sup>33</sup> And the prepared nanosheets are usually dispersed in polar solvents, like water, ethanol and ethylene glycol, which is great for lots of applications but still restricts their applications in some device fabrication processes, for example combination with semi-conducting polymer solutions. Recently solvent exchange method was also explored to disperse MoS<sub>2</sub> nanosheets in organic solvents.<sup>34</sup> Profound research is still needed to develop efficient liquid exfoliation procedures for MoS<sub>2</sub> nanosheets with good dispersion stability in wide range solvents, which can facilitate their applications for solution based device fabrication, such as spin coating, inkjet printing and role-to-role printing.

In the present work, alkylamines are introduced in the exfoliation system of MoS<sub>2</sub>. It was found that butylamine (BuA) in NMP can increase the production yield dramatically. Sonication time and alkyl chain length were explored in terms of production yield and colloidal stability of the MoS<sub>2</sub> nanosheets. More importantly, the produced MoS<sub>2</sub> nanosheets can be well dispersed in series of polar and nonpolar organic solvents with demonstrated stability for months. Hybrid polymer solar cell was constructed using polymer/fullerene/MoS<sub>2</sub> nanosheets mixture as the active layer for demonstrating its application potential in organic electronic devices.

## 2. EXPERIMENTAL DETAILS

### 2.1. Exfoliation of the MoS<sub>2</sub> Nanosheets

All chemicals mentioned below are purchased from Sigma-Aldrich if not specified and used without further purification. In a typical synthesis, 100 mg of MoS<sub>2</sub> powder (< 2 μm, 99%) were added to 10 mL of 10 vol% BuA and NMP mixed solution, which was stirred over night to allow the interaction of amine and MoS<sub>2</sub>. Then the dispersion was put in an ice water bath and sonicated for certain times using a point probe ultrasonic processor UP100H (100 W, 30 kHz) with Sonotrode MS3 made of titanium (tip diameter 3 mm) with on and off time of 9 s and 1 s. The amount of the MoS<sub>2</sub> powder, the type of alkylamine and sonication time (1 h to 8 h) were tuned to increase the exfoliation rate. Two starting concentrations of MoS<sub>2</sub> dispersions 10 and 50 mg mL<sup>-1</sup> were used and compared. Pure NMP without alkylamine, octylamine (Oca) and dodecylamine were also used to investigate the role of BuA and the effect of the alkyl chain length. Chemical structures of the used solvents and alkylamines are shown in Scheme 1. The production yield was doubled after introducing BuA to NMP and the concentration of MoS<sub>2</sub> nanosheets reached 19 mg mL<sup>-1</sup> after sonication for 8 h in BuA/NMP with the starting concentration of 50 mg mL<sup>-1</sup>.



**Scheme 1.** Chemical structures of the used solvents and alkylamines.

After sonication, the obtained black dispersions were centrifuged at 1500 rpm for 30 min to remove undesired large micro particles. Centrifugation at 1500 rpm or above gives dark green solutions, which are stable over months and can be diluted with toluene for UV-vis absorption measurement. To purify the MoS<sub>2</sub> nanosheets, the MoS<sub>2</sub>/NMP/BuA dispersions were mixed with chloroform and isopropanol and centrifuged at 4000 rpm for 15 min. Here isopropanol is a poor solvent used a lot to precipitate out nanocrystals capped with BuA. The MoS<sub>2</sub> nanosheets collected at the bottom of centrifuge tubes were washed with isopropanol and then redispersed in other solvents, such as dimethylformamide (DMF) or 1,2-dichlorobenzene (DCB) for further characterization and applications.

### 2.2. Characterization

UV-vis Absorption spectra were recorded using an Evolution 201 UV-vis Spectrophotometer (Thermo Scientific). Size and morphology of the nanosheets were studied using scanning electron microscopy (SEM) on a Quanta 200 FEGSEM with an accelerating voltage of 15 kV and transmission electron microscopy (TEM) using a Hitachi H7500 with an accelerating voltage of 100 kV. Raman spectra were recorded with a Renishaw Confocal Raman Microscope with a 514 nm laser.

### 2.3. Device Fabrication and Characterization

A pre-cleaned indium tin oxide (ITO) glass substrate was treated by ultraviolet-ozone for 10 min. Poly(3,4-ethylenedioxythiophene):poly(styrenesulfonate) (PEDOT:PSS) (Baytron-P 4083) buffer layer, with a thickness of 25 nm, was then spin coated onto the ITO substrates at 3000 rpm for 60 s and annealed at 130 °C for 30 min. Poly(3-hexylthiophene-2,5-diyl) (P3HT, from Rieke Metals) and [6,6]-Phenyl C<sub>61</sub> butyric acid methyl ester (PCBM, from Nano-C) were first dissolved in DCB to make 35 mg mL<sup>-1</sup> solution, respectively, followed by blending together in a ratio of 1:1 by weight. The P3HT:PCBM:MoS<sub>2</sub> (15:15:1 by weight) blend was prepared by blending the obtained 1 ml DCB solution of P3HT/PCBM with 0.2 ml of MoS<sub>2</sub> nanosheets DCB

solution (6 mg ml<sup>-1</sup>). The P3HT/PCBM/MoS<sub>2</sub> photoactive layer was fabricated by spin coating the blended solution at 800 rpm for 20 s, which gives a thickness of approximately 150 nm. After spin-coating, the thin films were dried slowly and then annealed at 110 °C for 10 mins for a better crystallinity.<sup>35</sup> Both the spin coating and thermal annealing of the photoactive layer were performed in N<sub>2</sub> atmosphere. After that a Ca/Al cathode (20/100 nm) was deposited by thermal evaporation in vacuum. The finalized device structure is ITO/PEDOT:PSS (25 nm)/P3HT:PCBM:MoS<sub>2</sub> (150 nm)/Ca (20 nm)/Al (100 nm). The working area was 0.075 cm<sup>2</sup> as defined by the overlapping of the ITO anode and Ca/Al cathode. The current–voltage curves were measured with a Keithley 2400 source meter under simulated sunlight of air mass 1.5 (100 mW cm<sup>-2</sup>).

### 3. RESULTS AND DISCUSSION

UV-vis absorption spectroscopy was used to monitor the exfoliation of the MoS<sub>2</sub> nanosheets, as shown in Figure 1. After sonication, a black dispersion of MoS<sub>2</sub>/BuA/NMP was obtained. It remains black after centrifuging at 500 rpm for 5 min and has strong scattering at long wavelength, indicating the existence of large sized particles. The two peaks at 617 and 676 nm can be assigned to the A<sub>1</sub> and B<sub>1</sub> absorption bands of MoS<sub>2</sub> resulted from the energy split valence band spin orbital coupling.<sup>29</sup> After further centrifuging at 3000 rpm for 5 min, the dispersion became dark green due to the removal of large lateral sized particles.<sup>27</sup> Both the two solution before centrifuging were obtained with the same initial MoS<sub>2</sub> concentration of 10 mg mL<sup>-1</sup>. Comparing the absorbance at 676 nm, we can see the increase from 0.26 to 0.51 after introducing 10 vol% BuA into NMP, indicating a doubled

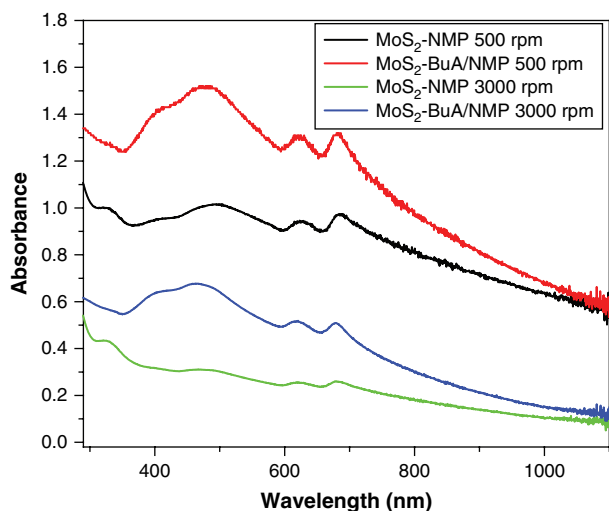


**Fig. 1.** UV-vis absorption spectra of the MoS<sub>2</sub> nanosheets (diluted 60 times) after sonication in NMP and 10 vol% BuA/NMP for 4 h with initial MoS<sub>2</sub> concentration of 10 mg mL<sup>-1</sup>.

exfoliation rate. In previous work, ligand conjugation of MoS<sub>2</sub> nanosheets has been reported using small molecules, such as thiols.<sup>36</sup> The alkylamines used here have been widely used to stabilize metal sulfide nanocrystals, either during or after synthesis. BuA is an excellent reagent for short chain ligand exchange, which forms stable quantum dot dispersion and can increase the electrical conductivity of the nanocrystals.<sup>37</sup> The amine group can act as electron donor<sup>38</sup> and the increased exfoliation rate by BuA can be attributed to the stronger interaction between MoS<sub>2</sub> nanosheets with the primary –NH<sub>2</sub> group in BuA, than that with NMP (see structures in Scheme 1).

The starting material used here is MoS<sub>2</sub> powder with average size less than 2 μm. Figure 2(a) shows the SEM image of the MoS<sub>2</sub> particles before sonication, which are composed of thick flakes and mostly have lateral size of 0.5–2 μm with a few of smaller ones. After sonication in BuA/NMP, few-layer thin nanosheets were obtained with lateral size of 200–300 nm or less as shown in Figure 2(b), which is consistent with previous studies of exfoliated MoS<sub>2</sub> nanosheets in NMP. On one hand, efforts have been mainly focused on large nanosheets of 300–700 nm towards device applications in previous researches. Here carefulness should be put to achieve the compromise of the increased exfoliation rate and the reduced lateral size. On the other hand, some much smaller nanosheets or nanocrystals were found with lateral size of few to tens of nanometers. The coexistence of nanosheets and small nanocrystals indicates that this method is potentially useful for preparing MoS<sub>2</sub> quantum dots (QDs) as novel luminescent<sup>39</sup> and energy conversion material considering that the analogue graphene QDs (or carbon QDs) have been widely used in photocatalysis, photovoltaics and bioimaging.<sup>40, 41</sup>

Raman spectroscopy was used for structure characterization of the exfoliated MoS<sub>2</sub> nanosheets. As shown in Figure 3, BuA capped MoS<sub>2</sub> nanosheets show two peaks at 380 and 405 cm<sup>-1</sup>, which can be ascribed to the E<sub>2g</sub> and A<sub>1g</sub> modes of exfoliated MoS<sub>2</sub>, respectively.<sup>42</sup> Compared with bulk MoS<sub>2</sub>, the smaller frequency difference (25 cm<sup>-1</sup>) between E<sub>2g</sub> and A<sub>1g</sub> modes in our MoS<sub>2</sub> nanosheets are consistent with previously reported results of 3–5 layer MoS<sub>2</sub> nanosheets.<sup>42</sup>

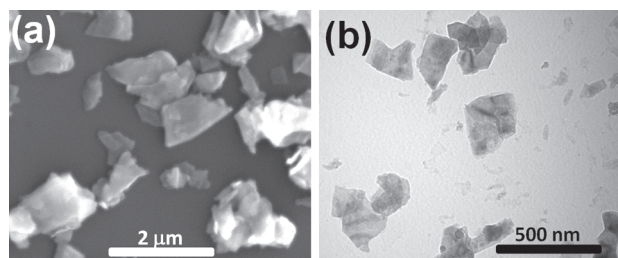


**Fig. 2.** (a) SEM image of the MoS<sub>2</sub> raw material without sonication and (b) TEM image of the MoS<sub>2</sub> nanosheets after sonication for 4 h in BuA/NMP.

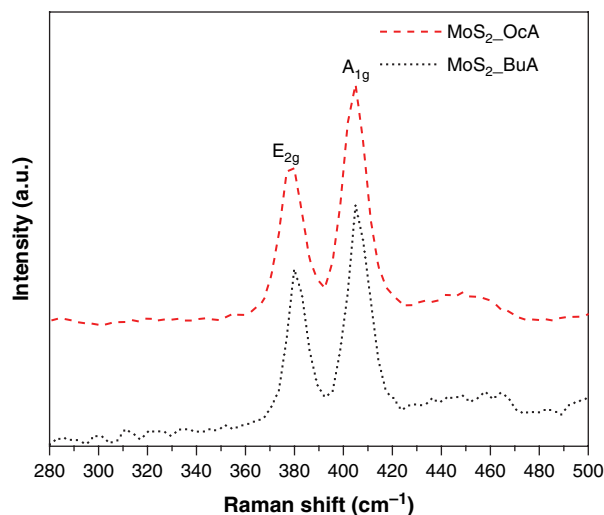


**Fig. 3.** Raman spectra of the exfoliated MoS<sub>2</sub> nanosheets after sonication in BuA/NMP (black dotted line) and OcA/DMF (red dashed line) for 4 h.

It was found that the very high exfoliation ratio enabled by the BuA is insensitive to the initial concentration, which is beneficial for high concentration dispersion of MoS<sub>2</sub> nanosheets. To achieve higher production yield, a modified recipe was used with 500 mg MoS<sub>2</sub> powder, 1 mL BuA and 9 mL NMP (initial concentration of 50 mg mL<sup>-1</sup>). Figure 4(a) shows the comparison of the absorption spectra after 4 h sonication with different starting MoS<sub>2</sub> amount. The sonicated dispersions were centrifuged at 1500 rpm for 30 min to remove large particles and then diluted 60 times with toluene for absorption measurement. With the initial MoS<sub>2</sub> concentration increased five times, the absorbance of the exfoliated MoS<sub>2</sub> nanosheets increased about four times from comparing the 612 and 672 nm peaks, and the BuA/NMP solution are capable for high concentration dispersion of MoS<sub>2</sub> nanosheets.

Sonication time is a key parameter to achieve high exfoliation ratio. Figure 4(b) shows the absorption spectra of the exfoliated MoS<sub>2</sub> nanosheets with increasing sonication time from 1 to 8 h. To get reliable absorbance values for comparison, the original dispersion was centrifuged at 1500 rpm and diluted 150 times with toluene. The inset in Figure 4(b) shows the absorbance increase at 455, 612 and 672 nm with increasing time. For example, the absorbance at 672 nm increases from 0.25 to 0.57 and 0.81 after 1 h, 4 h and 8 h sonication, indicating the efficient increase of exfoliation. The actual concentrations of the MoS<sub>2</sub> nanosheets after sonication 4 h and 8 h are 12 and 19 mg mL<sup>-1</sup>, respectively, estimated by weighting the dried nanosheets in 2 mL solution. It is not as high as 40 mg mL<sup>-1</sup> reported by O'neil et al. which was obtained by sonication of 100 mg mL<sup>-1</sup> MoS<sub>2</sub> for 144 h. However, it is worth to mention that our method achieved an exfoliation ratio of ~40% in 8 h by introducing BuA compared to 144 h in O'neil's work.<sup>28</sup>

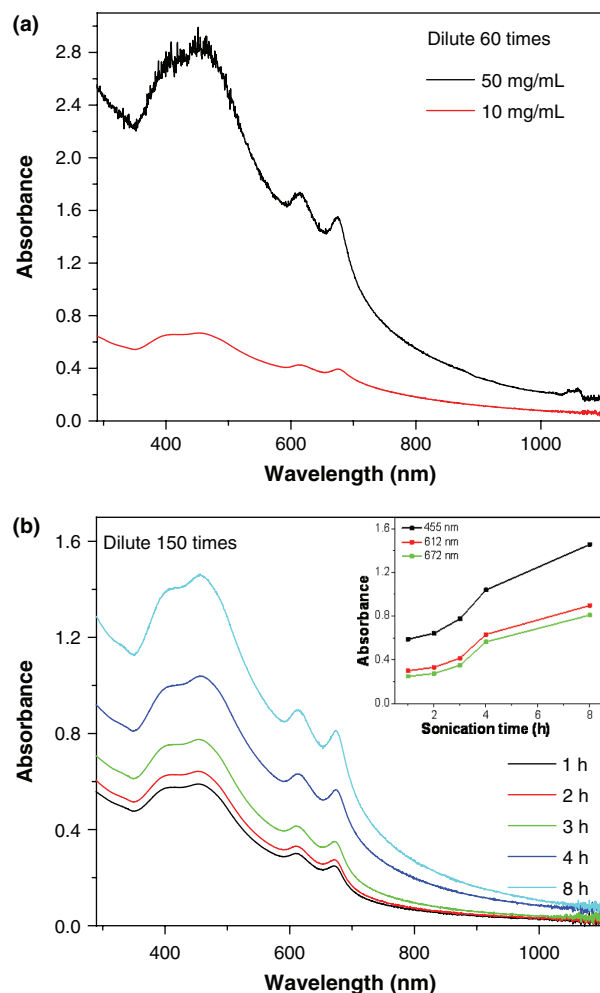


**Fig. 4.** UV-vis absorption spectra of the exfoliated MoS<sub>2</sub> nanosheets after sonication in 10 vol% BuA/NMP with different initial concentration of 10 and 50 mg mL<sup>-1</sup> (a) and for different time with 50 mg mL<sup>-1</sup> MoS<sub>2</sub> powder (b). The inset in panel (b) shows the absorbance increase at 455, 612 and 672 nm with increasing sonication time.

Among several amines with different alkyl chains, it was found that using BuA is much more efficient for the exfoliation than using other primary amines with longer alkyl chains, such as OcA and dodecylamine. This is because the mixture of MoS<sub>2</sub>, OcA and NMP cannot form a uniform dispersion as that in MoS<sub>2</sub>/NMP/BuA, though OcA and NMP are miscible with each other. The situation of dodecylamine is even worse that it is a solid at room temperature and has poor solubility in NMP. Replacing NMP with DMF to mix with OcA helps to improve the exfoliation yield due to better dispersion of the MoS<sub>2</sub> powder. However, the exfoliation yield in the OcA/DMF case is still ~30 times lower than that in the BuA/NMP case as indicated by the UV-vis absorption spectra (Fig. 5(a)). Although longer chain alkylamines are not good for exfoliation of the layered nanosheets, on the other hand the prepared MoS<sub>2</sub>-OcA nanosheets have higher colloidal stability in nonpolar solvent against centrifugation. The absorption spectra in Figure 5(b) show that there are

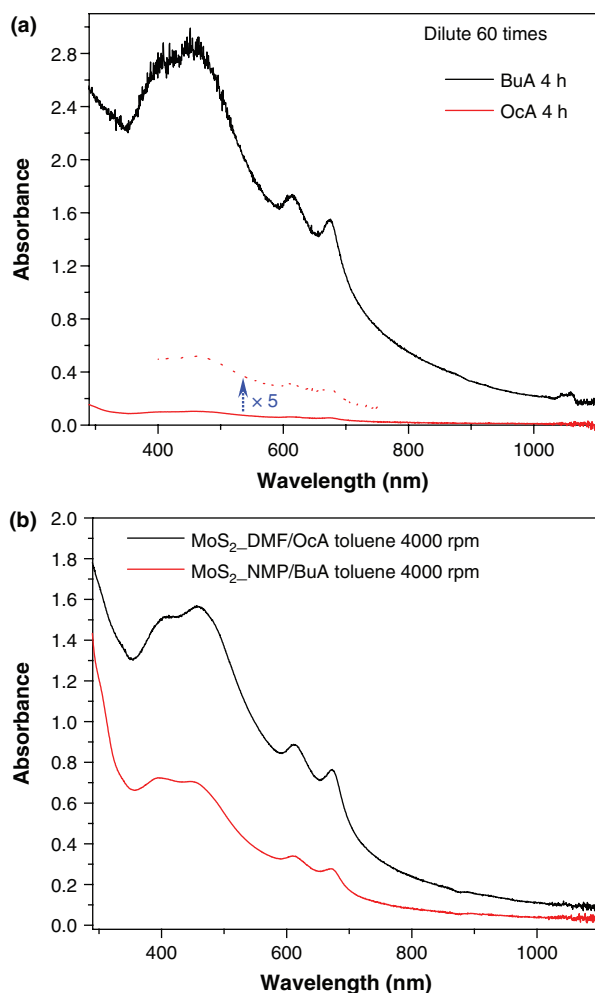


**Fig. 5.** (a) UV-vis absorption spectra of the MoS<sub>2</sub> nanosheets exfoliated in 10 vol% BuA/NMP and OcA/DMF after sonication for 4 h with initial MoS<sub>2</sub> amount of 50 mg mL<sup>-1</sup>. (b) UV-vis absorption spectra of the MoS<sub>2</sub> nanosheet dispersions after diluted with toluene and centrifuged at 4000 rpm for 30 min to examine the colloidal stability in nonpolar solvents.

more MoS<sub>2</sub> nanosheets in the OcA/DMF/toluene solution than BuA/NMP/toluene solution after centrifugation at 4000 rpm. We did not observe any obvious structural difference between the MoS<sub>2</sub> nanosheets exfoliated with BuA and OcA. OcA capped MoS<sub>2</sub> nanosheets also show two Raman peaks at 380 and 405 cm<sup>-1</sup> (Fig. 3), indicating the structure similarity of the exfoliated nanosheets, i.e., 3–5 layers. The result indicates that using amines with longer alkyl chains is potentially useful to improve their dispersion in nonpolar solvents.

The obtained nanosheets can be dispersed in common solvents, either polar or nonpolar, such as NMP, DMF, toluene, and DCB. In contrast, the MoS<sub>2</sub> nanosheets cannot form stable dispersion in water or isopropanol, which enables their cleaning by washing and centrifugation processes. Attractively, the nanosheet DCB dispersion is stable for months and is miscible with polymer and fullerene solutions at any ratio without any indication of

aggregation, which provides great opportunity for the solution process construction of organic and nano electronic devices.

MoS<sub>2</sub> nanosheets have attracted tremendous interests for energy conversion applications. It has been used as the active layer in MoS<sub>2</sub>/Au Schottky-barrier solar cells<sup>11</sup> and also as the interfacial layer in polymer solar cells.<sup>30</sup> It is well known that charge separation efficiency at the donor/acceptor interface is a critical issue for organic solar cells with high power conversion efficiency.<sup>35, 43–48</sup> To date, fullerene derivatives, such as PCBM and indene-C60 bisadduct (ICBA), are the most widely used *n*-type acceptor materials. Alternatively, *n*-type MoS<sub>2</sub> may also be a promising acceptor material due to their higher carrier mobility and larger electron Bohr radius than fullerene and its derivatives.<sup>49, 50</sup> Shanmugam et al. used MoS<sub>2</sub> nanosheets mixed with TiO<sub>2</sub> nanoparticles to increase the charge separation rate and conversion efficiency in TiO<sub>2</sub>/P3HT heterostructured solar cells.<sup>12</sup> Here the exfoliated MoS<sub>2</sub> nanosheets mixed with P3HT/PCBM in DCB with a final concentration ratio of 1:15:15 mg ml<sup>-1</sup> was used to construct hybrid organic solar cells with the structure of ITO/PEDOT:PSS/P3HT:PCBM:MoS<sub>2</sub>/Ca/Al as shown in Figure 6(a). Figure 6(b) shows the *I*–*V* curves of the solar cell, giving power conversion efficiency (PCE) of 1.03% and fill factor (FF) of 37.6%. It is worth to

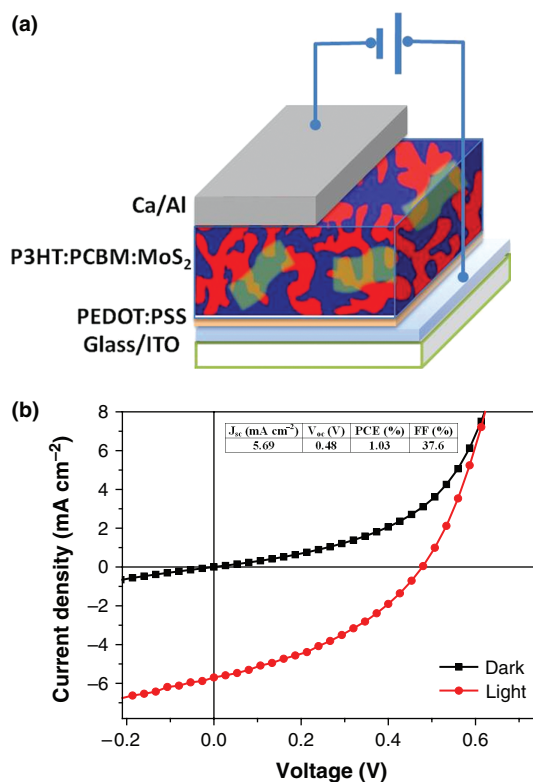


**Fig. 6.** (a) The schematic device structure of ITO/PEDOT:PSS/P3HT:PCBM:MoS<sub>2</sub>/Ca/Al; (b) dark and light *I*–*V* curves of the solar cell using MoS<sub>2</sub> nanosheets and polymer mixture as the active layer.

mention that the introduction of MoS<sub>2</sub> nanosheets resulted in lower FF and PCE compared to normal P3HT:PCBM solar cells without MoS<sub>2</sub>. This is due to the relatively large dark current (Fig. 6(b), black curve), which is probably caused by the high concentration of MoS<sub>2</sub> nanosheets. Further optimization is needed to achieve high efficiency solar cells using these MoS<sub>2</sub> nanosheets.

#### 4. CONCLUSIONS

In summary, we have explored the effect of alkylamines on the exfoliation of MoS<sub>2</sub> powder to produce MoS<sub>2</sub> nanosheets (3–5 layers) with point probe sonication. High exfoliation yield was obtained after introducing 10 vol% BuA into NMP which was doubled as compared to that in the absence of BuA. Further increase of the nanosheet exfoliation was achieved by increasing the starting MoS<sub>2</sub> concentration and the sonication time. Our results showed that the chain length of the alkylamines is an important issue for the high exfoliation yield of the layered nanosheets. Alkylamines can improve the colloidal stability of the nanosheets in nonpolar organic solvents, including DCB, over months. Hybrid solar cells employing P3HT:PCBM:MoS<sub>2</sub> nanosheets as photoactive layer has been demonstrated with a PCE of 1.03%.

**Acknowledgment:** Jinsong Huang acknowledges the financial support by the National Science Foundation under Awards ECCS-1201384 and ECCS-1252623, and Nebraska Public Power District through the Nebraska Center for Energy Sciences Research and Nebraska Research Initiative.

#### References and Notes

1. Q. H. Wang, K. Kalantar-Zadeh, A. Kis, J. N. Coleman, and M. S. Strano, *Nat. Nanotech.* 7, 699 (2012).
2. M. S. Xu, T. Liang, M. M. Shi, and H. Z. Chen, *Chem. Rev.* 113, 3766 (2013).
3. M. Chhowalla, H. S. Shin, G. Eda, L. J. Li, K. P. Loh, and H. Zhang, *Nat. Chem.* 5, 263 (2013).
4. S. Z. Butler, S. M. Hollen, L. Y. Cao, Y. Cui, J. A. Gupta, H. R. Gutierrez, T. F. Heinz, S. S. Hong, J. X. Huang, A. F. Ismach, E. Johnston-Halperin, M. Kuno, V. V. Plashnitsa, R. D. Robinson, R. S. Ruoff, S. Salahuddin, J. Shan, L. Shi, M. G. Spencer, M. Terrones, W. Windl, and J. E. Goldberger, *ACS Nano* 7, 2898 (2013).
5. D. Jariwala, V. K. Sangwan, L. J. Lauhon, T. J. Marks, and M. C. Hersam, *ACS Nano* 8, 1102 (2014).
6. B. Radisavljevic, A. Radenovic, J. Brivio, V. Giacometti, and A. Kis, *Nat. Nanotech.* 6, 147 (2011).
7. S. Kim, A. Konar, W. S. Hwang, J. H. Lee, J. Lee, J. Yang, C. Jung, H. Kim, J. B. Yoo, J. Y. Choi, Y. W. Jin, S. Y. Lee, D. Jena, W. Choi, and K. Kim, *Nat. Commun.* 3, 1011 (2012).
8. Z. Y. Yin, H. Li, H. Li, L. Jiang, Y. M. Shi, Y. H. Sun, G. Lu, Q. Zhang, X. D. Chen, and H. Zhang, *ACS Nano* 6, 74 (2012).
9. W. Choi, M. Y. Cho, A. Konar, J. H. Lee, G. B. Cha, S. C. Hong, S. Kim, J. Kim, D. Jena, J. Joo, and S. Kim, *Adv. Mater.* 24, 5832 (2012).
10. H. Li, Z. Y. Yin, Q. Y. He, H. Li, X. Huang, G. Lu, D. W. H. Fam, A. I. Y. Tok, Q. Zhang, and H. Zhang, *Small* 8, 63 (2012).
11. M. Shanmugam, C. A. Durcan, and B. Yu, *Nanoscale* 4, 7399 (2012).
12. M. Shanmugam, T. Bansal, C. A. Durcan, and B. Yu, *Appl. Phys. Lett.* 100, 153901 (2012).
13. Q. J. Xiang, J. G. Yu, and M. Jaroniec, *J. Am. Chem. Soc.* 134, 6575 (2012).
14. W. J. Zhou, Z. Y. Yin, Y. P. Du, X. Huang, Z. Y. Zeng, Z. X. Fan, H. Liu, J. Y. Wang, and H. Zhang, *Small* 9, 140 (2013).
15. M. Zhou, X. W. Lou, and Y. Xie, *Nano Today* 8, 598 (2013).
16. Z. B. Chen, D. Cummins, B. N. Reinecke, E. Clark, M. K. Sunkara, and T. F. Jaramillo, *Nano Lett.* 11, 4168 (2011).
17. C. F. Zhang, Z. Y. Wang, Z. P. Guo, and X. W. Lou, *ACS Appl. Mater. Interfaces* 4, 3765 (2012).
18. Y. F. Zhao, Y. X. Zhang, Z. Y. Yang, Y. M. Yan, and K. N. Sun, *Sci. Technol. Adv. Mater.* 14, 043501 (2013).
19. M. He, J. H. Jung, F. Qiu, and Z. Q. Lin, *J. Mater. Chem.* 22, 24254 (2012).
20. M. W. Lin, L. Z. Liu, Q. Lan, X. B. Tan, K. S. Dhindsa, P. Zeng, V. M. Naik, M. M. C. Cheng, and Z. X. Zhou, *Journal of Physics D-Applied Physics* 45, 345102 (2012).
21. K. K. Liu, W. J. Zhang, Y. H. Lee, Y. C. Lin, M. T. Chang, C. Su, C. S. Chang, H. Li, Y. M. Shi, H. Zhang, C. S. Lai, and L. J. Li, *Nano Lett.* 12, 1538 (2012).
22. D. Kong, H. Wang, J. J. Cha, M. Pasta, K. J. Koski, J. Yao, and Y. Cui, *Nano Lett.* 13, 1341 (2013).
23. Z. Y. Zeng, Z. Y. Yin, X. Huang, H. Li, Q. Y. He, G. Lu, F. Boey, and H. Zhang, *Angew. Chem., Int. Ed. Engl.* 50, 11093 (2011).
24. J. Zheng, H. Zhang, S. Dong, Y. Liu, C. T. Nai, H. S. Shin, H. Y. Jeong, B. Liu, and K. P. Loh, *Nat. Commun.* 5, 2995 (2014).
25. V. Nicolosi, M. Chhowalla, M. G. Kanatzidis, M. S. Strano, and J. N. Coleman, *Science* 340, 1420 (2013).
26. A. Ciesielski and P. Samori, *Chem. Soc. Rev.* 43, 381 (2014).
27. J. N. Coleman, M. Lotya, A. O'Neill, S. D. Bergin, P. J. King, U. Khan, K. Young, A. Gaucher, S. De, R. J. Smith, I. V. Shvets, S. K. Arora, G. Stanton, H. Y. Kim, K. Lee, G. T. Kim, G. S. Duesberg, T. Hallam, J. J. Boland, J. J. Wang, J. F. Donegan, J. C. Grunlan, G. Moriarty, A. Shmeliov, R. J. Nicholls, J. M. Perkins, E. M. Grieveson, K. Theuwissen, D. W. McComb, P. D. Nellist, and V. Nicolosi, *Science* 331, 568 (2011).
28. A. O'Neill, U. Khan, and J. N. Coleman, *Chem. Mater.* 24, 2414 (2012).
29. Y. G. Yao, L. Tolentino, Z. Z. Yang, X. J. Song, W. Zhang, Y. S. Chen, and C. P. Wong, *Adv. Func. Mater.* 23, 3577 (2013).
30. M. A. Ibrahim, T. W. Lan, J. K. Huang, Y. Y. Chen, K. H. Wei, L. J. Li, and C. W. Chu, *RSC Adv.* 3, 13193 (2013).
31. U. Halim, C. R. Zheng, Y. Chen, Z. Y. Lin, S. Jiang, R. Cheng, Y. Huang, and X. F. Duan, *Nat. Commun.* 4, 2213 (2013).
32. R. J. Smith, P. J. King, M. Lotya, C. Wirtz, U. Khan, S. De, A. O'Neill, G. S. Duesberg, J. C. Grunlan, G. Moriarty, J. Chen, J. Z. Wang, A. I. Minett, V. Nicolosi, and J. N. Coleman, *Adv. Mater.* 23, 3944 (2011).
33. J. Q. Liu, Z. Y. Zeng, X. H. Cao, G. Lu, L. H. Wang, Q. L. Fan, W. Huang, and H. Zhang, *Small* 8, 3517 (2012).
34. Z. Tang, Q. Wei, and B. Guo, *Chem. Commun.* 50, 3934 (2014).
35. Y. B. Yuan, T. J. Reece, P. Sharma, S. Poddar, S. Ducharme, A. Gruverman, Y. Yang, and J. S. Huang, *Nat. Mater.* 10, 296 (2011).
36. S. S. Chou, M. De, J. Kim, S. Byun, C. Dykstra, J. Yu, J. X. Huang, and V. P. Dravid, *J. Am. Chem. Soc.* 135, 4584 (2013).
37. J. P. Clifford, G. Konstantatos, K. W. Johnston, S. Hoogland, L. Levina, and E. H. Sargent, *Nat. Nanotech.* 4, 40 (2009).
38. S. Mourdikoudis and L. M. Liz-Marzan, *Chem. Mater.* 25, 1465 (2013).
39. V. Stengl and J. Henych, *Nanoscale* 5, 3387 (2013).
40. H. T. Li, Z. H. Kang, Y. Liu, and S. T. Lee, *J. Mater. Chem.* 22, 24230 (2012).

41. H. T. Li, X. D. He, Z. H. Kang, H. Huang, Y. Liu, J. L. Liu, S. Y. Lian, C. H. A. Tsang, X. B. Yang, and S. T. Lee, *Angew. Chem., Int. Ed. Engl.* 49, 4430 (2010).
42. H. Li, Q. Zhang, C. C. R. Yap, B. K. Tay, T. H. T. Edwin, A. Olivier, and D. Baillargeat, *Adv. Func. Mater.* 22, 1385 (2012).
43. G. Li, V. Shrotriya, J. S. Huang, Y. Yao, T. Moriarty, K. Emery, and Y. Yang, *Nat. Mater.* 4, 864 (2005).
44. T. M. Clarke and J. R. Durrant, *Chem. Rev.* 110, 6736 (2010).
45. Z. G. Xiao, Q. F. Dong, P. Sharma, Y. B. Yuan, B. D. Mao, W. J. Tian, A. Gruverman, and J. S. Huang, *Adv. Energy Mater.* 3, 1581 (2013).
46. Y. B. Yuan, P. Sharma, Z. G. Xiao, S. Poddar, A. Gruverman, S. Ducharme, and J. S. Huang, *Energy Environ. Sci.* 5, 8558 (2012).
47. Y. Yuan, Z. Xiao, B. Yang, and J. Huang, *J. Mater. Chem. A* 2, 6027 (2014).
48. B. Yang, Y. B. Yuan, P. Sharma, S. Poddar, R. Korlacki, S. Ducharme, A. Gruverman, R. F. Saraf, and J. S. Huang, *Adv. Mater.* 24, 1455 (2012).
49. H. Y. Li, B. C. K. Tee, J. J. Cha, Y. Cui, J. W. Chung, S. Y. Lee, and Z. N. Bao, *J. Am. Chem. Soc.* 134, 2760 (2012).
50. R. Doolen, R. Laitinen, F. Parsapour, and D. F. Kelley, *J. Phys. Chem. B* 102, 3906 (1998).

Received: 25 March 2014. Accepted: 1 April 2014.